sustained response to interferon therapy. Ann Intern Med. 2000; 132: 517-524.

12) Poynard T, McHutchison J, Davis GL, Esteban-Mur R, Goodman Z, Bedossa P, Albrecht J. Impact of interferon alfa-2b and ribavirin on progression of liver fibrosis in patients with chronic hepatitis C. Hepatology 2000; 32: 1131-1137.

13) Xu L, Hui AY, Albanis E, Arthur MJ, O'Byrne SM, Blaner WS, Mukherjee P, Friedman SL, Eng FJ. Human hepatic stellate cell lines, LX-1 and LX-2: new tools for analysis of hepatic fibrosis. Gut 2005; 54: 142-151.

14) Saile B, Matthes N, Knittel T, Ramadori G. Transforming growth factor beta and tumor necrosis factor alpha inhibit both apoptosis and proliferation of activated rat hepatic stellate cells. Hepatology 1999; 30, 196-202.

15) Takaoka A, Hayakawa S, Yanai H, Stoiber D, Negishi H, Kikuchi H, Sasaki S, Imai K, Shibue T, Honda K, Taniguchi T, Integration of interferon-alpha/beta signalling to p53 responses in tumour suppression and antiviral defence. Nature 2003; 424: 516-523.

16) Hadziyannis SJ, Sette H Jr, Morgan TR, Balan V, Diago M, Marcellin P, Ramadori G, Bodenheimer H Jr, Bernstein D, Rizzetto M, Zeuzem S, Pockros PJ, Lin A, Ackrill AM; PEGASYS International Study Group. Peginterferon-alpha2a and ribavirin combination therapy in chronic hepatitis C: a randomized study of treatment duration and ribavirin dose. Ann Intern Med. 2004; 140: 346-355.

17) Manns MP, Wedemeyer H, Cornberg M. Treating viral hepatitis C: efficacy, side effects, and complications. Gut. 2006; 55: 1350-1359.

18) Hoofnagle JH, Seeff LB. Peginterferon and ribavirin for chronic hepatitis C. N Engl J Med. 2006; 355: 2444-51.

19) Gale M Jr, Foy EM. Evasion of intracellular host defence by hepatitis C virus. Nature. 2005; 436: 939-945.

20) Nishiguchi S, Shiomi S, Nakatani S, Takeda T, Fukuda K, Tamori A, Habu D, Tanaka T, Prevention of hepatocellular carcinoma in patients with chronic active hepatitis C and cirrhosis. Lancet. 2001; 357: 196-197

21) Yoshida H, Arakawa Y, Sata M, Nishiguchi S, Yano M, Fujiyama S, Yamada G, Yokosuka O, Shiratori Y, Omata M. Interferon therapy prolonged life expectancy among chronic hepatitis C patients. Gastroenterology 2002; 123: 483-491.

22) Shiratori Y, Ito Y, Yokosuka O, Imazeki F, Nakata R, Tanaka N, Arakawa Y, Hashimoto E, Hirota K, Yoshida H, Ohashi Y, Omata M; Tokyo-Chiba Hepatitis Research Group. Antiviral therapy for cirrhotic hepatitis C: association with reduced hepatocellular carcinoma development and improved survival. Ann Intern Med. 2005; 142: 105-114.

23) Kondo M, Nagano H, Wada H, Damdinsuren B, Yamamoto H, Hiraoka N, Eguchi H, Miyamoto A, Yamamoto T, Ota H, Nakamura M, Marubashi S, Dono K, Umeshita K, Nakamori S, Sakon M, Monden M. Combination of IFN-alpha and 5-fluorouracil induces apoptosis through IFN-alpha/beta receptor in human hepatocellular carcinoma cells. Clin Cancer Res. 2005; 11: 1277-1286.

24) Eguchi H, Nagano H, Yamamoto H,

Miyamoto A, Kondo M, Dono K, Nakamori S, Umeshita K, Sakon M, Monden M. Augmentation of antitumor activity of 5-fluorouracil by interferon alpha is associated with up-regulation of p27Kip1 in human hepatocellular carcinoma cells. Clin Cancer Res. 2000; 6: 2881-2890.

25) Tiggelman AM, Boers W, Linthorst C, Sala M, Chamuleau RA,. Collagen synthesis by human liver (myo)fibroblasts in culture: evidence for a regulatory role of IL-1 beta, IL-4, TGF beta and IFN gamma. J Hepatol. 1995; 23: 307-317.

26) Rockey DC, Maher JJ, Jarnagin WR, Gabbiani G, Friedman SL. Inhibition of rat hepatic lipocyte activation in culture by interferon-gamma. Hepatology 1992; 16: 776-784.

27) Sakaida I, Uchida K, Matsumura Y, Okita K. Interferon gamma treatment prevents procollagen gene expression without affecting transforming growth factor-beta1 expression in pig serum-induced rat liver fibrosis in vivo. J Hepatol. 1998; 28: 471-479.

28) Baroni GS, D'Ambrosio L, Curto P, Casini A, Mancini R, Jezequel AM, Benedetti A. Interferon gamma decreases hepatic stellate cell activation and extracellular matrix deposition in rat liver fibrosis. Hepatology 1996; 23: 1189-1199.

29) Mallat A, Preaux AM, Blazejewski S, Rosenbaum J, Dhumeaux D, Mavier P. Interferon alfa and gamma inhibit proliferation and collagen synthesis of human Ito cells in culture. Hepatology 1995; 21: 1003-1010.

30) Inagaki Y, Nemoto T, Kushida M, Sheng Y, Higashi K, Ikeda K, Kawada N, Shirasaki F, Takehara K, Sugiyama K, Fujii M, Yamauchi H, Nakao A, de Crombrugghe B, Watanabe T, Okazaki I. Interferon alfa down-regulates collagen gene transcription and suppresses experimental hepatic fibrosis in mice. Hepatology 2003; 38: 890-899.

31) Novo E, Marra F, Zamara E, Valfre di Bonzo L, Monitillo L, Cannito S, Petrai I, Mazzocca A, Bonacchi A, De Franco RS, Colombatto S, Autelli R, Pinzani M, Parola M., Overexpression of Bcl-2 by activated human hepatic stellate cells: resistance to apoptosis as a mechanism of progressive hepatic fibrogenesis in humans. Gut 2006; 55: 1174-1182.

Legends for Figures

Figure 1. Effect of IFNα on [^{3}H]thymidine incorporation in HSC. Sub-confluent HSC were cultured on plastic dishes for 3 days in 10% FBS/DMEM, and then maintained for 24 h in serum-free DMEM. These cells were successively stimulated with IFNα for 24 h, and then pulse-labeled with 1.0 μCi/ml of [^{3}H]thymidine during the last 24 h. The incorporated radioactivity was counted by liquid scintillation. * $p < 0.01$.

Figure 2. Effect of IFNα on PDGF-BB-stimulated [^{3}H]thymidine incorporation in HSC. Sub-confluent HSC were cultured on plastic dishes for 3 days in 10% FBS/DMEM, and then maintained for 24 h in serum-free DMEM. These cells were successively stimulated with PDGF-BB (10 ng/ml) in the presence or absence of IFNα for 24

h, and then were pulse-labeled with 1.0 μCi/ml of [^{3}H]thymidine during the last 24 h. The incorporated radioactivity was counted by liquid scintillation. * $p < 0.01$.

Figure 3. Effects of IFNα on cell cycle-related protein expression and the activation of MEK, MAPK, and Akt stimulated with PDGF-BB in HSC. (A) Expression of cyclin D1, cdk2, cdk4, cdk6, p27, p21, and p53 was determined by immunoblot. (B) Expression of PDGFRβ, phospho-MEK, total MEK, phospho-MAPK, total MAPK, phospho-Akt, and total Akt in HSC under PDGF-BB (10 ng/ml) stimulation was analyzed by immunoblot.

Figure 4. Effect of IFNα and TNFα on number of HSC. HSC were maintained on plastic culture plates in DMEM supplemented with 10% fetal bovine serum. Then, the medium was replaced by serum-free DMEM with IFNα and/or TNFα and the culture was continued for another 48 h. Numbers of HSC were determined by the Alamar blue assay (BIOSOURCE) according to the manufacturer's instructions. * $p < 0.01$.

Figure 5. Effect of IFNα and TNFα on the cell number of HSC. HSC were maintained on plastic culture plates in DMEM supplemented with 10% fetal bovine serum. Then, the medium was replaced by serum-free DMEM with IFNα and/or TNFα and the culture was continued for another 48 h. Cell appearance of HSC were determined under a microscope at a magnification of x 200. Note that the cell number was markedly decreased by incubating them with IFNα plus TNFα. IFNα: 100 IU/ml. TNFα: 10 ng/ml.

Figure 6. DNA fragmentation of HSC treated with IFNα and TNFα.
Isolated DNA was loaded onto a 1.5% agarose gel containing ethidium bromide, electrophoresed in Tris acetate/EDTA buffer for 2 hours at 50 V, and photographed under ultraviolet illumination. Note that treatment of HSC with IFNα plus TNFα induced DNA flagmentation.
IFNα: 100 IU/ml. TNFα: 10 ng/ml.

Figure 7. Flow cytometric quantification of apoptosis in LX-2 treated with IFNα or TNFα, IFNα/TNFα.
LX-2 cells were maintained on plastic culture plates in DMEM supplemented with 10% FBS. Then, the medium was replaced by serum-free DMEM with IFNα and/or TNFα and the culture was continued for another 48 h. The data show the percental portion of apoptotic cells per total LX-2 population using flow cytometry. *$p < 0.05$; **$p < 0.01$.

Figure 8. Apoptosis-related protein expressions in HSC. (A) The cytochrome C content in the cytosol and mitochondria was determined by Western blot. (B) The activation of caspase-3 was studied by detecting the amount of cleaved caspase-3. (C) Expression of CAD and ICAD in HSC treated with IFNα and/or TNFα.
IFNα: 100 IU/ml. TNFα: 10 ng/ml.

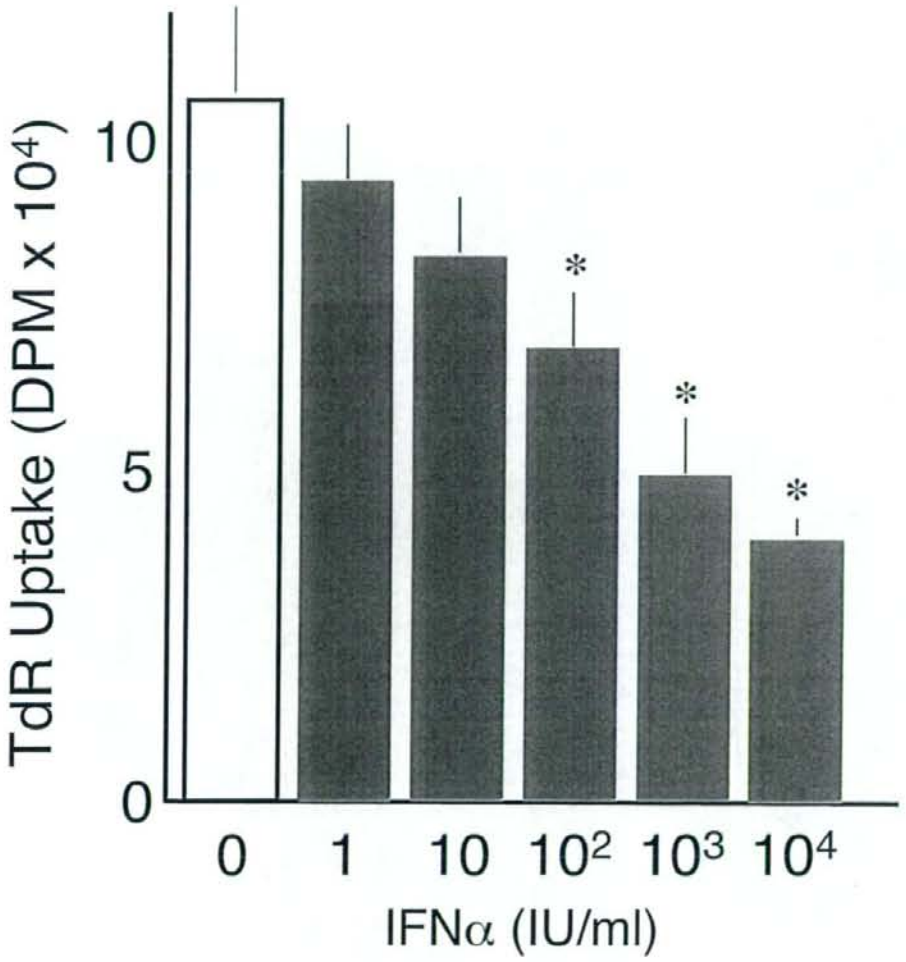

Ogawa T et al. Figure 1

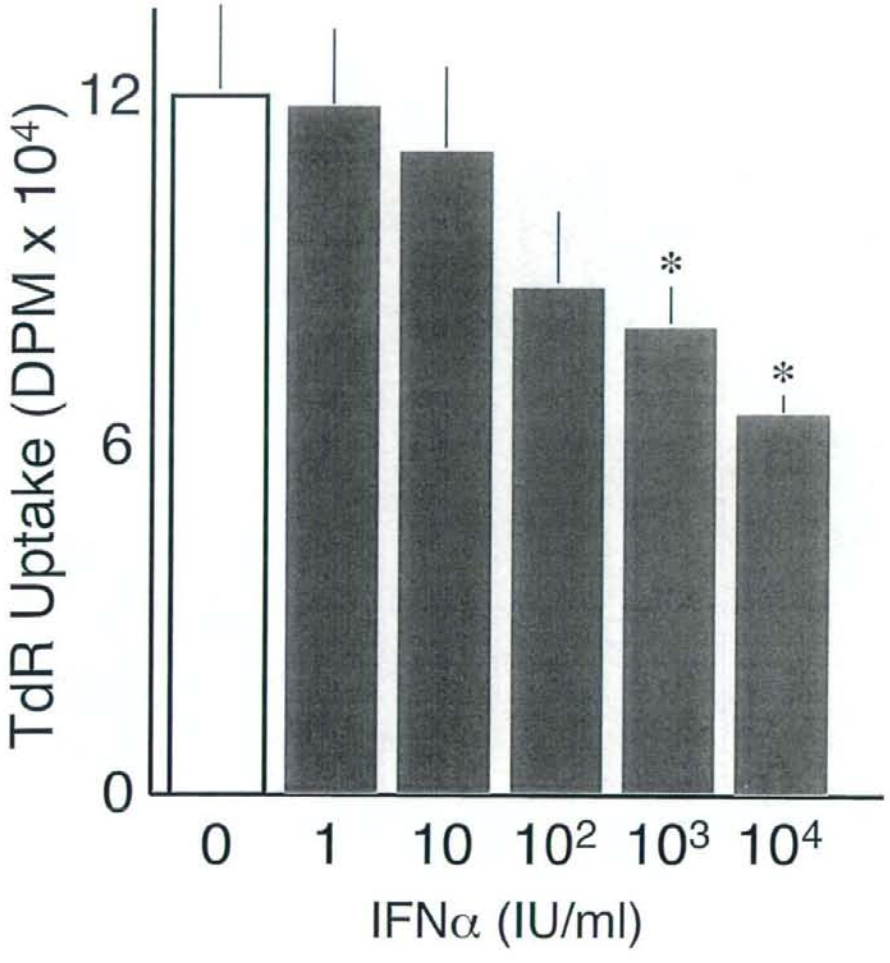

Ogawa T et al. Figure 2

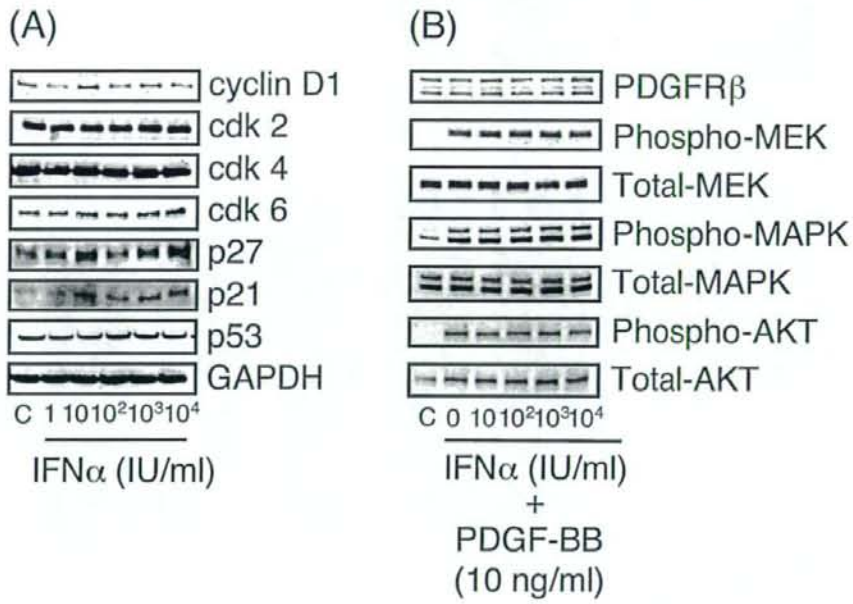

Ogawa T et al. Figure 3

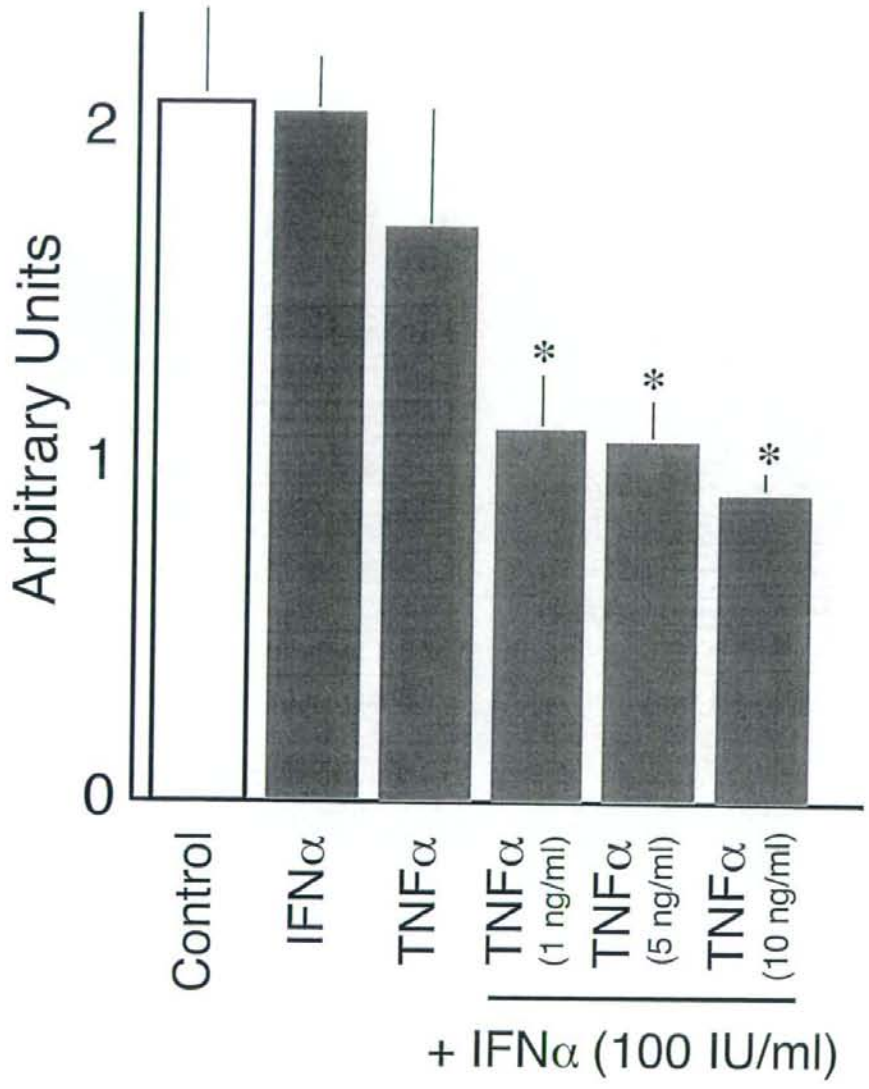

Ogawa T et al. Figure 4

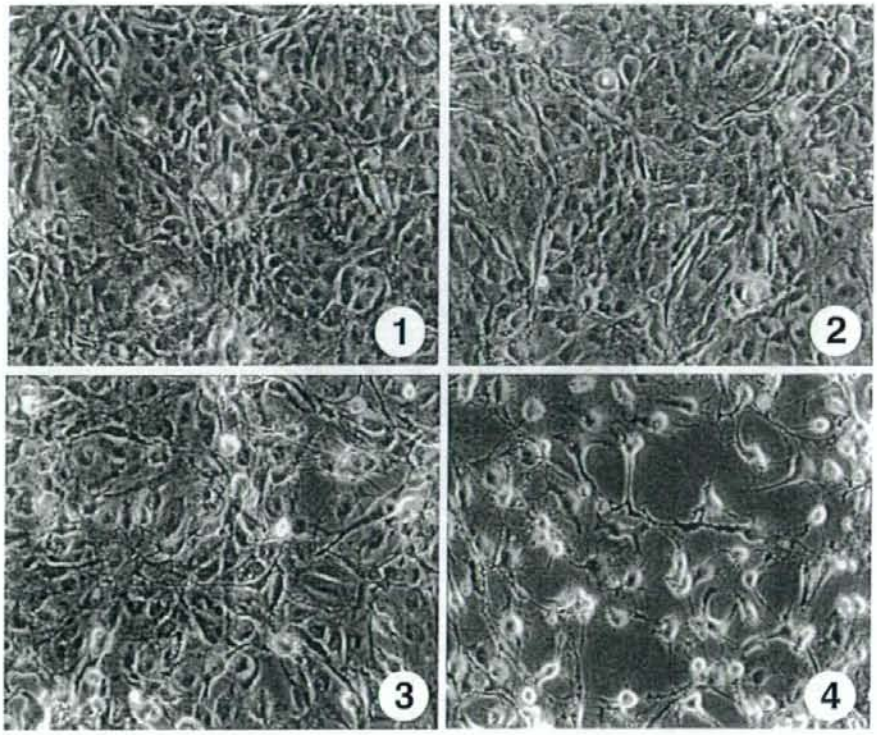

Ogawa T et al. Figure 5

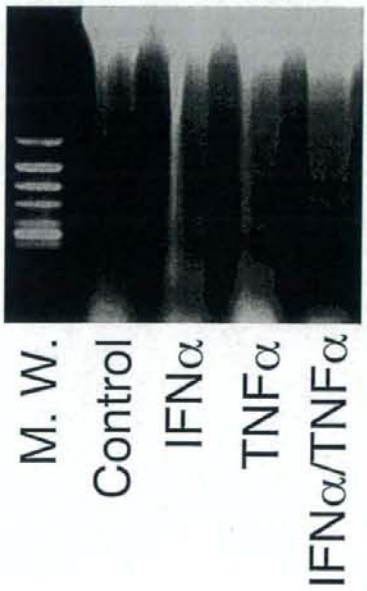

Ogawa T et al. Figure 6

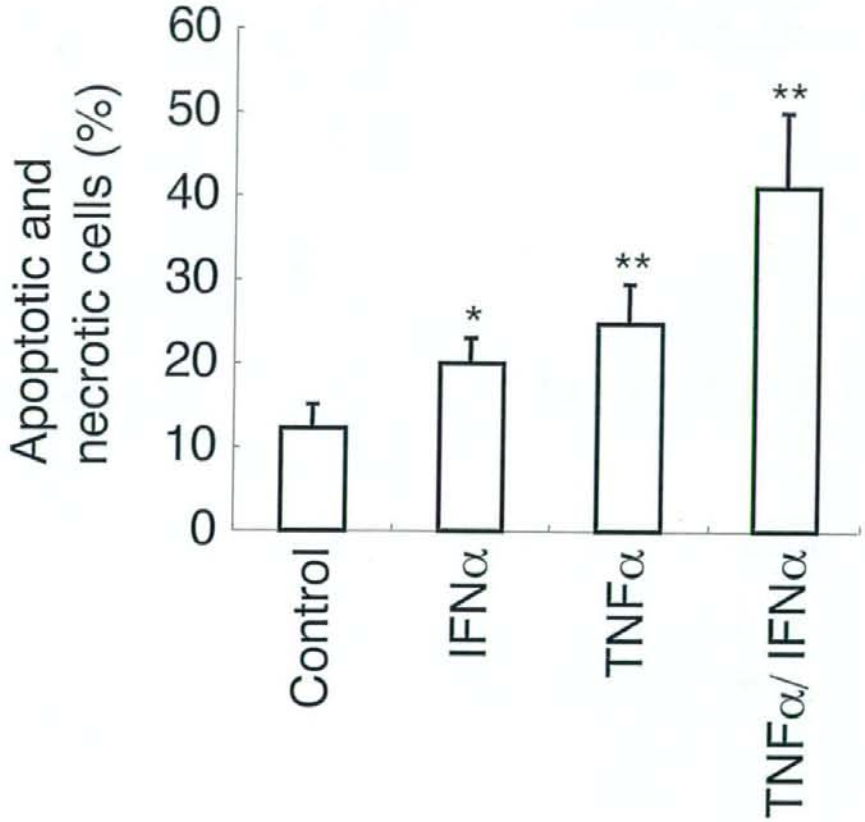

Ogawa T et al. Figure 7

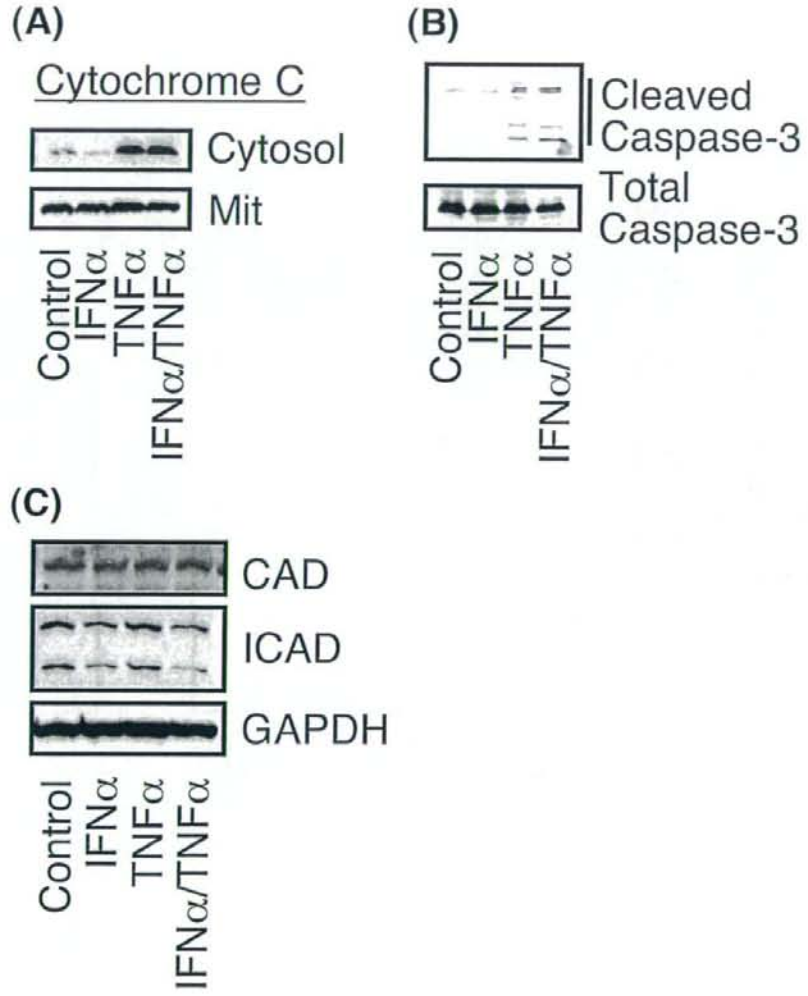

Ogawa T et al. Figure 8

Hepatol Int
DOI 10.1007/s12072-008-9113-y

ORIGINAL ARTICLE

Induction of tropomyosin during hepatic stellate cell activation and the progression of liver fibrosis

Kohji Otogawa · Tomohiro Ogawa · Ryoko Shiga · Kazuo Ikeda · Norifumi Kawada

Received: 13 August 2008 / Accepted: 30 October 2008

Abstract The activation of hepatic stellate cells (HSCs) is a cue to initiate liver fibrosis. Activated stellate cells acquire contractile activity similar to pericytes and myofibroblasts in other organs by inducing the contractile machinery of cytoskeletons such as smooth muscle α-actin (α-SMA), a well-known marker of activated stellate cells, and actin-binding proteins. We further show herein the expression of tropomyosin in rat HSCs in the course of their activation during primary culture and liver tissue damaged by thioacetamide intoxication. In immunoblot analysis, tropomyosin became detectable in an early stage of the primary culture of rat stellate cells in a manner similar to the expression of α-SMA and platelet-derived growth factor receptor-β. Tropomyosin was found to be colocalized with α-SMA on fluorescent immunocytochemistry. At the liver tissue level, an increased expression of tropomyosin was observed by immunoblot analysis and immunohistochemistry along the septum of fibrosis, where α-SMA was enriched. These results strongly suggest that tropomyosin is a new marker of activated stellate cells and may serve as a useful diagnostic marker of liver fibrosis.

Keywords Actin · Cell contraction · Vitamin A · Liver injury · Liver sinusoid

K. Otogawa · T. Ogawa · N. Kawada (✉)
Department of Hepatology, Graduate School of Medicine, Osaka City University, 1-4-3, Asahimachi, Abeno, Osaka 545-8585, Japan
e-mail: kawadanori@med.osaka-cu.ac.jp

R. Shiga · K. Ikeda
Department of Anatomy, Graduate School of Medicine, Osaka City University, Osaka, Japan

Abbreviations

DMEM	Dulbecco's modified Eagle's medium
ECM	Extracellular matrix
GAPDH	Glyceraldehyde-3-phosphate dehydrogenase
HSC	Hepatic stellate cell
PBS	Phosphate-buffered saline
PCR	Polymerase chain reaction
PDGFR-β	Platelet-derived growth factor receptor-β
TAA	Thioacetamide
α-SMA	Smooth muscle-α actin

Introduction

Hepatic stellate cells (HSCs) play a key role in liver fibrogenesis regardless of the pathogenesis [1–4]. In response to local tissue damage and hepatocyte necrosis, HSCs undergo activation characterized by the proliferation, migration, contraction, secretion of several profibrogenic mediators such as cytokines, growth factors, chemokines, and tissue inhibitors of matrix metalloproteinases, and generation of extracellular matrix (ECM) materials such as type I collagen. HSC activation thus contributes to scar formation in chronically injured liver tissue.

One of the indicators of activated HSCs is smooth muscle α-actin (α-SMA), the actin isoform typical of smooth muscle cell differentiation [5–10]. Similar to the expression of γ-actin, α-SMA was first demonstrated in primary-cultured rat HSCs in the course of the culture-dependent HSC activation process [5]. α-SMA-positive HSCs are also seen along the fibrotic septum of chronically damaged livers of rodent models, in which ECM proteins such as type I collagen and fibronectin are dominantly produced and deposited [11, 12]. Furthermore, in the human liver, the augmented expression of α-SMA has been

Published online: 10 December 2008

documented in and around the area of hepatocyte damage [13, 14].

Tropomyosin is one of the actin-associated proteins, present in virtually all eukaryotic cells, and modulates the interaction between actin and myosin to stabilize the actin-filament structure. Tropomyosin assembles into an α-helical coiled heterodimer composed of an α-chain and a β-chain, with each molecule interacting with six or seven monomers of actin [15, 16]. Tropomyosin regulates the contractility of striated muscle by blocking myosin-binding sites on actin in the relaxed state. On activation, tropomyosin moves away from these sites [17]. X-ray studies have suggested that the initiation of smooth muscle contraction leads to the movement of tropomyosin in a manner similar to that in striated muscle [18]. Although one recent study has shown the expression and organization of actin filaments and tropomyosin in the cloned hepatic GRX cell line [19], tropomyosin expression patterns in primary cultured HSCs and the fibrotic liver remain to be studied.

This study aimed to demonstrate the presence of tropomyosin in HSCs and clarify the dynamics of its expression pattern during HSC activation. Herein, we report in detail the expression pattern of tropomyosin in cultured rat HSCs and fibrotic liver tissue induced in rats by thioacetamide (TAA) administration, and further demonstrate the network of α-SMA filaments and tropomyosin in primary HSC cultures.

Materials and methods

Materials

Collagenase was purchased from Wako Pure Chemical Co. (Osaka, Japan). Pronase E was obtained from Merck (Damstadt, Germany). Mouse monoclonal IgG2a antibody against α-SMA, mouse monoclonal IgG1 antibody against tropomyosin, Dulbecco's modified Eagle's medium (DMEM), TAA, and fetal bovine serum (FBS) were purchased from Sigma Chemical Co. (Saint Louis, MO, USA). Rabbit polyclonal IgG antibodies against human platelet-derived growth factor receptor-β (PDGFR-β) that reacts with rat PDGFR-β were purchased from Santa Cruz Biotechnology (Santa Cruz, CA, USA). Horseradish peroxidase-conjugated secondary antibodies against mouse and rabbit immunoglobulins were obtained from Dako. Alexa Fluor 488 goat antimouse IgG2a antibodies and Alexa Fluor 594 goat antimouse IgG1 antibodies were from Molecular Probes (Eugene, OR, USA). ECL immunoblotting detection reagent was purchased from Amersham Pharmacia Biotech (Buckinghamshire, England). Immobilon P membranes were from Millipore Corp. (Bedford, MA, USA). Cell culture inserts were from Falcon (Beckton Dickinson, Franklin Lakes, NJ, USA). All the other reagents were purchased from Sigma Chemical Co. or Wako Pure Chemical Co.

Animals

Pathogen-free male Wistar rats (12-week-old, body weight 200–220 g) were obtained from SLC (Shizuoka, Japan). Animals were housed at a constant temperature and supplied with laboratory chow and water ad libitum. The protocol of the experiments was approved by the Animal Research Committee of Osaka City University (Guide for Animal Experiments, Osaka City University).

Induction of liver fibrosis

Liver fibrosis was induced in rats ($n = 3$) by the intraperitoneal injection of TAA (40 mg/body weight) dissolved in 2 ml of saline twice a week for up to 10 weeks. Control rats ($n = 3$) were given 2 ml of saline during the same period.

Preparation of HSCs

HSCs were isolated from male Wistar rats, as previously described in detail [20]. Isolated HSCs were suspended in DMEM supplemented with 10% FBS at a cell density of 5×10^5 cells/ml, and 1.5 ml of the cell suspension was introduced into a 35-mm cell tissue culture plate (Falon, 3003). After the culture had continued for the indicated number of days, the cells were fixed in 4% paraformaldehyde solution for immunocytochemistry or lysed for immunoblotting.

Immunoblotting

Protein samples (10 μg) were subjected to SDS-PAGE and then transferred onto Immobilon P membranes. After blocking, the membranes were treated with primary antibodies and then with peroxidase-conjugated secondary antibodies. Immunoreactive bands were visualized using the ECL system (Amersham Pharmacia Biotech) and documented by LAS 1000 (Fuji Photo Film, Kanagawa, Japan). The density of bands was analyzed using a BIO-RAD GS-700 densitometer. Experiments were repeated thrice using samples obtained from HSCs isolated from different rats.

Immunohistochemistry and collagen staining

Immunohistochemistry was performed using the methods described in detail elsewhere [21]. After the development of fibrosis, rats were anesthetized and laparotomized. The

liver was perfused with phosphate-buffered saline (PBS) and then perfusion-fixed with 4% formaldehyde, dehydrated, and embedded in Polybed. Sections were cut at a thickness of 5 μm and stained for 1 h in 0.1% (w/v) Sirius red (Direct Red 80, Aldrich, Milwaukee, WI, USA) [22]. Double immunostaining analysis was carried out using methods described previously [22]. After blocking with 5% bovine serum albumin/PBS, they were incubated overnight with primary antibodies in the medium. They were then incubated with both 20 μg/ml Alexa Fluor 488 goat anti-mouse IgG2a antibody and 20 μg/ml Alexa Fluor 594 goat anti-mouse IgG1 antibody for 2 h. Specimens were counterstained for nuclei with DAPI. The sections were observed under an LSM510 confocal laser scanning microscope (Carl Zeiss, Germany).

Cultured HSCs on glass microscope slides were fixed with 3.7% formaldehyde for 30 min at room temperature. After washing thrice with PBS containing 0.1% Triton X-100, the fixed cells were incubated with anti-α-SMA antibody and anti-tropomyosin antibody for 1 h at room temperature and successively with FITC-labeled goat antimouse IgG1 (Alexa Fluor 488) and rhodamine-labeled goat antimouse IgG2a (Alexa Fluor 594) for 1 h at room temperature. After washing, the specimens were observed under an LSM510 confocal laser scanning microscope (Carl Zeiss, Germany). Experiments were repeated thrice using samples obtained from HSCs isolated from different rats.

Immunohistochemical analysis of human liver samples

One specimen obtained by resection during surgery from subjects with normal liver function was used as a control. Informed written consent was obtained from all patients at the time of their liver biopsy, and the study was conducted in conformance with the Helsinki Declaration. The diagnosis of liver cirrhosis was established on the basis of the clinical and histopathological features. Immunohistochemistry was performed according to the methods described above.

Results

Tropomyosin expression in primary cultured HSCs

We investigated the expression of tropomyosin in primary-cultured HSCs as a model because HSC culture precisely resembles the in vivo cellular phenotypic change of HSCs from a vitamin A-storing quiescent phenotype to an activated and myofibroblastic phenotype in response to inflammatory stimuli [23]. Freshly isolated and plated HSCs resembled lipocytes, extended branching cytoplasmic processes, and enclosed multiple droplets that contained retinol (Fig. 1Aa). After culturing for 3 days, the cells expanded their cell body with enlarged processes and nuclei, and the size of fat droplets decreased (Fig. 1Ab). By

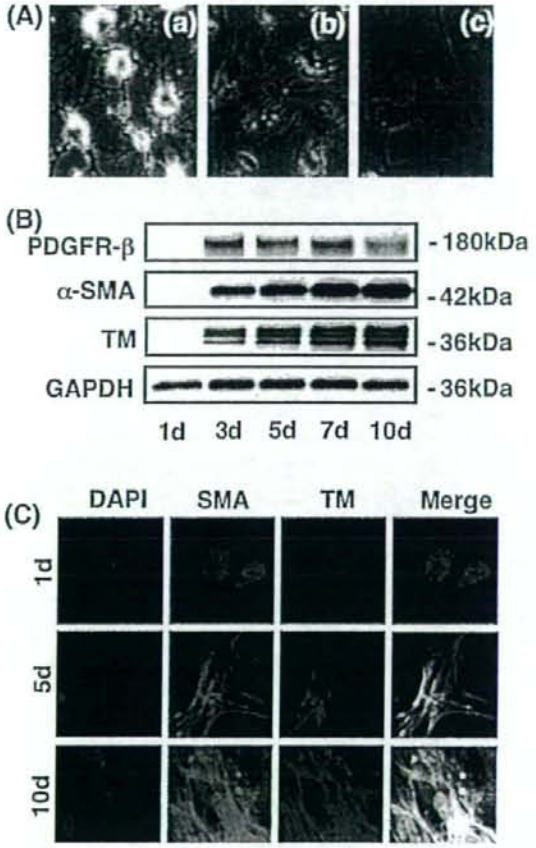

Fig. 1 Tropomyosin expression in primary cultured HSCs. **A** The cell morphology of isolated and cultured HSCs was observed under phase-contrast microscopy everyday, monitored, and digitally recorded. **a** Day 1. HSCs attached to the plate enclose droplets that contain vitamin A. **b** Day 3. HSCs start extending their processes. **c** Day 7. HSCs showed enlarged cell body and lose their droplets (magnification, ×200). **B** The expression of tropomyosin in cultured HSCs was determined by immunoblot and immunocytochemistry. Whole-cell homogenates were subjected to SDS-PAGE, transferred onto the membrane, and successively immunoreacted with PDGFR-β, α-SMA, or tropomyosin. Note that tropomyosin is induced in HSCs time dependently after starting the culture in a manner similar to the expression of PDGFR-β and α-SMA. Representative data from three independent preparations are presented here. **C** Immunocytochemistry of tropomyosin and α-SMA. Cultured HSCs on days 1, 5, and 10 were fixed in 4% paraformaldehyde and subjected to immunocytochemistry, as described in section "Materials and methods". Note that tropomyosin appears on day 5 and becomes prominent on day 10. Tropomyosin colocalizes and generates stress fibers with α-SMA (magnification ×200)

day 7, most of the cells had lost their fat droplets, spread more prominently, and appeared "myofibroblastic" (Fig. 1Ac). These observations are in good agreement with previous reports [1, 6, 21].

As shown in Fig. 1B, immunoblot analysis showed that bands for tropomyosin at molecular weights of 36–39 kDa [24] were invisible in freshly isolated HSCs, started to appear in them after being cultured for 3 days, and thereafter increased in a time-dependent manner. The relative level of tropomyosin evaluated by densitometric normalization against GAPDH gradually increased with culture prolongation (data not shown). The multiple bands detected are considered to be related to post-transcriptional modification, particularly N-terminal acetylation, of the protein, as described elsewhere [25]. Tropomyosin induction took place in a similar manner to that of α-SMA and PDGFR-β (Fig. 1B). These observations were further confirmed by immunocytochemistry. α-SMA became readily detectable on day 1 and was uniformly distributed in the cytoplasm. HSCs cultured for more than 5 days exhibited a flattened and stretched morphology with developed stress fibers, which consisted of α-SMA (Fig. 1C). Tropomyosin was negligible on day 1, but was visible and co-localized with α-SMA at day 5, and then exhibited prominent stress fibers crossing the cytoplasm together with α-SMA bundles (Fig. 1C).

Expression of tropomyosin in fibrotic livers

Tropomyosin induction in culture-activated HSCs prompted us to investigate its expression in liver tissue. As shown in Fig. 2A, total protein extracted from rat livers treated with TAA for 6 or 10 weeks cross-hybridized to α-SMA and tropomyosin antibodies, whereas virtually no hybridization was observed in the total extraction from an intact rat liver. This result indicates that tropomyosin is not ubiquitously expressed in liver-constituent cells such as hepatocytes, Kupffer cells, and endothelial cells. The level of tropomyosin in the liver homogenate increased in a time-dependent manner after TAA administration, similar to the induction of PDGFR-β and α-SMA. Collagen deposition was prominent in the liver after a 10-week TAA administration, as shown on Sirius red staining. Tropomyosin was found to be present along the fibrotic septum, although it was rarely seen in the intact liver (Fig. 2B). Double immunostaining of α-SMA and tropomyosin confirmed that these two proteins co-existed in and around the fibrotic septum and were hardly present in "pseudolobular" parenchyma where no fibrosis was obvious (Fig. 2C). However, activated HSCs that were present close to the septum and positive for α-SMA also expressed tropomyosin (Fig. 2C, high), indicating both activated HSCs and septum-forming myofibroblasts ubiquitously expressed

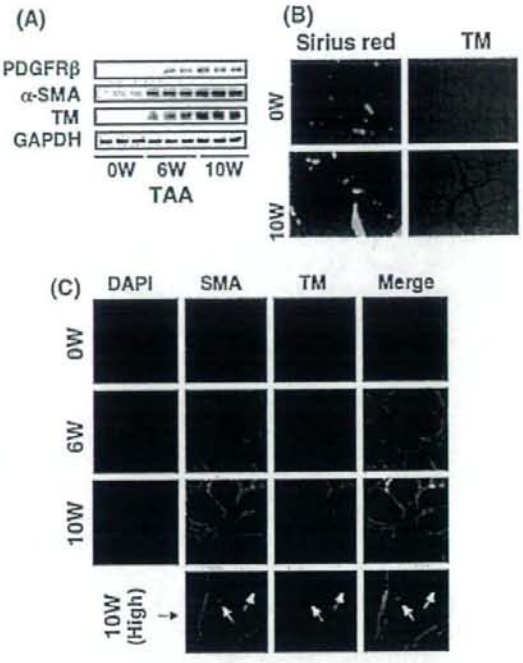

Fig. 2 Expression of tropomyosin in fibrotic livers. The expression of tropomyosin in the fibrotic liver was determined by immunoblot and immunohistochemistry. **A** Whole-liver homogenates were subjected to SDS-PAGE, transferred onto the membrane, and successively immunoreacted with PDGFR-β, α-SMA, or tropomyosin. Note that tropomyosin is induced in the liver of rats treated with TAA time dependently after starting injection in a similar manner to the expression of PDGFR-β and α-SMA. **B** Histology. Prominent liver fibrosis is observed in the liver of rats treated with TAA for 10 weeks by Sirius red staining. Tropomyosin expression is clear along the septa. **C** Fluorescent immunohistochemistry of tropomyosin and α-SMA. Double immunostaining was performed in the liver of rats treated with TAA for 6 and 10 weeks. Note that both proteins always colocalize and are expressed strongly at the site between noninjurious parenchyma and septa (magnification ×100). Activated HSCs (*arrows*) that were present close to the septum and positive for α-SMA also expressed tropomyosin (magnification ×400)

tropomyosin. A strong linear-pattern expression of these proteins at the site between the septum and the parenchyma was notable. Tropomyosin expression was rarely observed in intact human liver, while it was localized along the fibrotic septum in human cirrhosis (Fig. 3).

Discussion

Activated HSCs express α-SMA as contractile machinery. Although accumulated studies have evaluated the importance of α-SMA and other cytoskeletons filaments on HSC contraction, there has been no report on the expression of tropomyosin, which is one of the components of actin

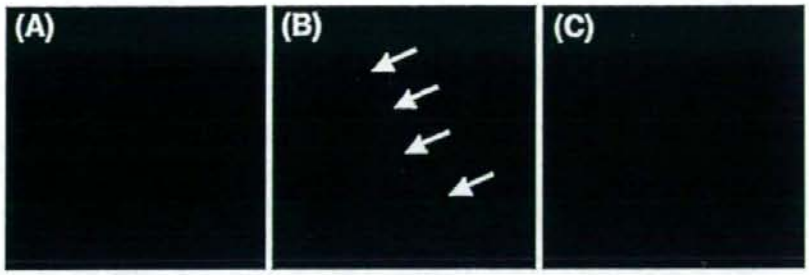

Fig. 3 Expression of tropomyosin in human livers. The expression of tropomyosin in the human liver was determined by immunohistochemistry. **A** Intact human liver. **B** Cirrhosis caused by hepatitis C infection. **C** Negative control stained without antitropomyosin antibody (magnification ×200)

filaments and calcium-binding proteins and plays a major role in the contraction process of smooth muscle, in HSCs and fibrotic liver tissue. The key molecular function of tropomyosin is to shield and unshield the binding site of myosin to actin [15, 16]. Thus, tropomyosin is speculated to play a pivotal role also in the contraction of HSCs. In the present study, we report for the first time that the expression of tropomyosin is found predominantly in activated HSCs and to be as high as α-SMA. These observations suggest that tropomyosin is a regulatory protein which counteracts or triggers the contraction of HSCs due to its calcium-binding status. In fact, HSC contraction is reportedly induced by endothelin-1, angiotensin II, and thrombin, which are all intracellular calcium inducers [23].

HSCs are considered to be more contractile at presinusoidal terminal portal venules in the injured liver, as indicated by the high-level expression of endothelin-1 receptors [26]. HSCs localized at this site also generate endothelin-1 and angiotensin-II, that are responsible molecules for portal hypertension, a pathological process induced by constriction of the hepatic vasculature [27, 28]. As a consequence, tropomyosin expressed at the site between the septum and the parenchyma is speculated to play a positive regulatory role in actin–myosin association and contribute to presinusoidal portal rigidity.

In conclusion, the present findings indicate that tropomyosin could be a novel marker for activated HSCs in vivo as well as in culture and be utilizable for a clinical diagnosis of liver fibrosis.

Acknowledgment This work was supported by the Grants-in-Aid from the Japan Society for the Promotion of Science to NK.

References

1. Blomhoff R, Wake K. Perisinusoidal stellate cells of the liver: important roles in retinol metabolism and fibrosis. FASEB J 1991;5:271–277
2. Friedman SL. Seminars in medicine of the Beth Israel Hospital, Boston. The cellular basis of hepatic fibrosis. Mechanisms and treatment strategies. N Engl J Med 1993;328:1828–1835. doi:10.1056/NEJM199306243282508
3. Okuyama H, Shimahara Y, Kawada N. The hepatic stellate cell in the post-genomic era. Histol Histopathol 2002;17:487–495
4. Bataller R, Brenner DA. Hepatic stellate cells as a target for the treatment of liver fibrosis. Semin Liver Dis 2001;21:437–451. doi:10.1055/s-2001-17558
5. Ramadori G, Veit T, Schwögler S, Dienes HP, Knittel T, Rieder H, et al. Expression of the gene of the alpha-smooth muscle-actin isoform in rat liver and in rat fat-storing (ITO) cells. Virchows Arch 1990;59:349–357
6. Kawada N, Klein H, Decker K. Eicosanoid-mediated contractility of hepatic stellate cells. Biochem J 1992;285:367–371
7. Rockey DC, Boyles JK, Gabbiani G, Friedman SL. Rat hepatic lipocytes express smooth muscle actin upon activation in vivo and in culture. J Submicrosc Cytol Pathol 1992;24:193–203
8. Rockey DC, Housset CN, Friedman SL. Activation-dependent contractility of rat hepatic lipocytes in culture and in vivo. J Clin Invest 1993;92:1795–1804. doi:10.1172/JCI116769
9. Kawada N, Tran-Thi TA, Klein H, Decker K. The contraction of hepatic stellate (Ito) cells stimulated with vasoactive substances. Possible involvement of endothelin 1 and nitric oxide in the regulation of the sinusoidal tonus. Eur J Biochem 1993;213:815–823. doi:10.1111/j.1432-1033.1993.tb17824.x
10. Skalli O, Ropraz P, Trzeciak A, Benzonana G, Gillessen D, Gabbiani G. A monoclonal antibody against alpha-smooth muscle actin: a new probe for smooth muscle differentiation. J Cell Biol 1986;103:2787–2796. doi:10.1083/jcb.103.6.2787
11. Bhunchet E, Wake K. Role of mesenchymal cell populations in porcine serum-induced rat liver fibrosis. Hepatology 1992;16:452–1473. doi:10.1002/hep.1840160623
12. Rockey DC, Chung JJ. Endothelin antagonism in experimental hepatic fibrosis. Implications for endothelin in the pathogenesis of wound healing. J Clin Invest 1996;98:1381–1388. doi:10.1172/JCI118925
13. Sakaida I, Nagatomi A, Hironaka K, Uchida K, Okita K. Quantitative analysis of liver fibrosis and stellate cell changes in patients with chronic hepatitis C after interferon therapy. Am J Gastroenterol 1999;94:489–496. doi:10.1111/j.1572-0241.1999.884_m.x
14. Martinelli AL, Ramalho LN, Zucoloto S. Hepatic stellate cells in hepatitis C patients: relationship with liver iron deposits and severity of liver disease. J Gastroenterol Hepatol 2004;19:91–98. doi:10.1111/j.1440-1746.2004.03255.x
15. Hitchcock-DeGregori SE, Varnell TA. Tropomyosin has discrete actin-binding sites with sevenfold and fourteenfold periodicities. J Mol Biol 1990;214:885–896. doi:10.1016/0022-2836(90)90343-K
16. McLachlan AD, Stewart M. The troponin binding region of tropomyosin. Evidence for a site near residues 197 to 127. J Mol Biol 1976;106:1017–1022. doi:10.1016/0022-2836(76)90349-1
17. Lehrer SS. The regulatory switch of the muscle thin filament: Ca21 or myosin heads? J Muscle Res Cell Motil 1994;15:232–236. doi:10.1007/BF00123476

18. Vibert PJ, Haselgrove JC, Lowy J, Poulsen FR. Structural changes in actin-containing filaments of muscle. J Mol Biol 1972;71:757–767. doi:10.1016/S0022-2836(72)80036-6
19. Mermelstein CS, Guma FC, Mello TG, Fortuna VA, Guaragna RM, Costa ML, et al. Induction of the lipocyte phenotype in murine hepatic stellate cells: reorganisation of the actin cytoskeleton. Cell Tissue Res 2001;306:75–83. doi:10.1007/s004410100428
20. Kristensen DB, Kawada N, Imamura K, Miyamoto Y, Tateno C, Seki S, et al. Proteome analysis of rat hepatic stellate cells. Hepatology 2000;32:268–277. doi:10.1053/jhep.2000.9322
21. Nakatani K, Okuyama H, Shimahara Y, Saeki S, Kim DH, Nakajima Y, et al. Cytoglobin/STAP, its unique localization in splanchnic fibroblast-like cells and function in organ fibrogenesis. Lab Invest 2004;84:91–101. doi:10.1038/sj.labinvest.3700013
22. Nakatani K, Seki S, Kawada N, Kitada T, Yamada T, Sakaguchi H, et al. Expression of SPARC by activated hepatic stellate cells and its correlation with the stages of fibrogenesis in human chronic hepatitis. Virchows Arch 2002;441:466–474. doi:10.1007/s00428-002-0631-z
23. Kawada N. The hepatic perisinusoidal stellate cell. Histol Histopathol 1997;12:1069–1080
24. Somara S, Bitar KN. Tropomyosin interacts with phosphorylated HSP27 in agonist-induced contraction of smooth muscle. Am J Physiol Cell Physiol 2004;286:C1290–C1301. doi:10.1152/ajpcell.00458.2003
25. Gondo K, Ueno T, Sakamoto M, Sakisaka S, Sata M, Tanikawa K. The endothelin-1 binding site in rat liver tissue: light- and electron-microscopic autoradiographic studies. Gastroenterology 1993;104:1745–1749
26. Rockey DC, Weisiger RA. Endothelin induced contractility of stellate cells from normal and cirrhotic rat liver: implications for regulation of portal pressure and resistance. Hepatology 1996;24:233–240. doi:10.1002/hep.510240137
27. Pinzani M, Milani S, De Franco R, Grappone C, Caligiuri A, Gentilini A, et al. Endothelin 1 is overexpressed in human cirrhotic liver and exerts multiple effects on activated hepatic stellate cells. Gastroenterology 1996;110:534–548. doi:10.1053/gast.1996.v110.pm8566602
28. Bataller R, Sancho-Bru P, Gines P, Brenner DA. Liver fibrogenesis: a new role for the renin-angiotensin system. Antioxid Redox Signal 2005;7:1346–1355. doi:10.1089/ars.2005.7.1346

Liver International ISSN 1478-3223

REVIEW ARTICLE

Hepatic sinusoidal cells in health and disease: update from the 14th International Symposium

Bård Smedsrød[1], David Le Couteur[2], Kenichi Ikejima[3], Hartmut Jaeschke[4], Norifumi Kawada[5], Makoto Naito[6], Percy Knolle[7], Laura Nagy[8], Haruki Senoo[9], Fernando Vidal-Vanaclocha[10] and Noriko Yamaguchi[9]

1 Department of Cell Biology and Histology, Institute of Medical Biology, University of Tromsø, Tromsø, Norway
2 Centre for Education and Research on Ageing, University of Sydney and Concord RG Hospital, Sydney, NSW, Australia
3 Department of Gastroenterology, Juntendo University School of Medicine, Tokyo, Japan
4 Department of Pharmacology, Toxicology & Therapeutics, University of Kansas Medical Center, Kansas City, KS, USA
5 Department of Hepatology, Graduate School of Medicine, Osaka City University, Osaka, Japan
6 Department of Cellular Function, Division of Cellular and Molecular Pathology, Niigata University Graduate School of Medical and Dental Sciences, Niigata, Japan
7 Institute for Molecular Medicine and Experimental Immunology, Friedrich-Wilhelms-University Bonn, Bonn, Germany
8 Department of Nutrition, Case Western Reserve University, Cleveland, OH, USA
9 Department of Cell Biology and Histology, Akita University School of Medicine, Akita, Japan
10 Department of Cellular Biology and Histology, Basque Country University School of Medicine, Bizkaia, Spain

Keywords
hepatic stellate cell – Kupffer cell – liver – liver sinusoidal endothelial cell – sinusoid

Correspondence
Prof. Bård Smedsrød, Department of Cell Biology and Histology, Institute of Medical Biology, University of Tromsø, NO-9037 Tromsø, Norway
Tel: +47 7764 4687/+47 9959 9463
Fax: +47 7764 5400
e-mail: bard.smedsrod@fagmed.uit.no

Received 6 December 2008
Accepted 25 December 2008

DOI:10.1111/j.1478-3231.2009.01979.x

Abstract
This review aims to give an update of the field of the hepatic sinusoid, supported by references to presentations given at the 14th International Symposium on Cells of the Hepatic Sinusoid (ISCHS2008), which was held in Tromsø, Norway, August 31–September 4, 2008. The subtitle of the symposium, 'Integrating basic and clinical hepatology', signified the inclusion of both basal and applied clinical results of importance in the field of liver sinusoidal physiology and pathophysiology. Of nearly 50 oral presentations, nine were invited tutorial lectures. The authors of the review have avoided writing a 'flat summary' of the presentations given at ISCHS2008, and instead focused on important novel information. The tutorial presentations have served as a particularly important basis in the preparation of this update. In this review, we have also included references to recent literature that may not have been covered by the ISCHS2008 programme. The sections of this review reflect the scientific programme of the symposium (http://www.ub.uit.no/munin/bitstream/10037/1654/1/book.pdf):
1. Liver sinusoidal endothelial cells.
2. Kupffer cells.
3. Hepatic stellate cells.
4. Immunology.
5. Tumor/metastasis.
Symposium abstracts are refered to by a number preceded by the letter A.

Liver sinusoidal endothelial cells

Fenestrations

In his key note lecture (A1), Eddie Wisse underlined the fact that electron microscopy is still the only method of observing fenestrations in the liver sinusoidal endothelial cells (LSEC) and that sinusoidal cells of different mammalian species are amazingly similar in fine structure. He further provided information that pore size varies among species and strains and between periportal and perivenous areas of the sinusoid. After isolation, the porosity of LSECs decreases from approximately 10% at 6 h to 1% at 48 h (1) (A9). Porosity is influenced by the isolation techniques (2), the culture conditions and the presence of vascular endothelial growth factors (VEGFs) (3). Potential LSEC lines such as SKHep1 (4) might overcome some of these issues. Fenestrations are supported by actin cytoskeletal filaments, and disruption of the cytoskeleton is associated with a dramatic increase in porosity. Cellular signals involved in the regulation of actin, such as cortactin and transforming growth factor (TGF)-β1 (A15), and the Rho-like GTPases (5) influence porosity. VEGF produced by hepatocytes is probably the key cytokine involved in the regulation of LSEC fenestration mediated by actions on VEGF-R2 expressed on LSEC (6). The role of fenestrations in the bi-directional transfer of substrates between hepatocytes and sinusoidal blood is now well established (7) (A1, 13). Defenestration impairs the hepatic disposition of lipoproteins, albumin-bound drugs and other particulate substrates (7, 8) (A11, A13) and potentially impacts on T-cell interactions with hepatocytes (9). In studies using adenoviral delivery of transgene DNA, uptake of the transgene in hepatocytes correlated strongly with the LSEC pore size. The size of the adenovirus particle is 93 nm, with protruding fibres of 30 nm. Thus, the use of adenoviral-mediated gene therapy in humans may be difficult owing to the small LSEC pore size (103–107 nm) (10).

Scavenger function

Endocytic rate and capacity of LSECs are probably the highest known of any cell type in the human body. Peter McCourt presented an update on endocytosis receptors in these cells (A2). The cells carry three major types of endocytosis receptors to keep the blood clean.

The liver sinusoidal endothelial cell mannose receptor

It is known that mannose receptor (MR) clearance of several blood-borne soluble macromolecules carrying mannose in the ultimate position is carried out mainly in the LSECs, but not in the Kupffer cells (KCs) (11). Studies including MR-deficient knockout (KO) mice showed that the clearance of denatured collagen is MR mediated (12). Using the same KO mice showed that LSEC MR mediates the import of blood-borne lysosomal enzymes for re-use in the endo/lysosomal apparatus (13).

The liver sinusoidal endothelial cell scavenger receptor

Previous studies established that blood-borne negatively charged soluble macromolecular scavenger receptor (SR) ligands are cleared mainly by endocytosis in LSECs (14, 15). Hyaluronan and chondroitin sulphate, which are negatively charged connective tissue polysaccharides believed to be cleared by a highly specific hyaluronan receptor, are taken up by the same SRs that take up aminoterminal propeptides of type I and III procollagen (16). Studies employing KO mice lacking SR-A showed that the LSEC SR is distinct from SR-A (17). Recent evidence indicates that the major LSEC SR is represented by the two closely related receptors, stabilin-1 and -2 (18).

The liver sinusoidal endothelial cell Fc-γ receptor IIb2 (IIb2)

Of the known Fc-γ receptors, only IIb2 is able to mediate endocytosis of immune complexes (ICs) and only IIb2 is expressed in LSECs. Clark Anderson noted that the presence of this receptor in LSECs has, astonishingly, been ignored by immunologists (A4). Trond Berg (A5) reported that ICs endocytosed via IIb2 are degraded at a lower rate than antigens endocytosed via LSEC SR (19). Moreover, the ICs are associated with lipid rafts after cross-linking before internalization via clathrin-coated pits, and a large proportion of the internalized ICs is recycled back to the plasma membrane. Both these events delay receptor–ligand transport to later endocytic compartments. Cross-linking of LSEC IIb2 does not lead to tyrosine phosphorylation. It was suggested that the LSEC IIb2, similar to its role in dendritic cells, is able to present antigens to B-cells (A4). IIb2 in LSECs and placenta endothelium may share a similar role in local vascular immunity (20).

Comparative aspects of scavenger function

Liver sinusoidal endothelial cells represent the mammalian counterpart of vertebrate scavenger endothelial cells (SEC) (21). Using highly efficient clathrin-mediated endocytosis, these cells clear an array of colloids and soluble macromolecules from the circulation, whereas macrophages use phagocytosis to remove particles of size > 200 nm. Martin–Armas (A7) presented a study on SR-mediated endocytosis of immune-stimulating bacterial oligonucleotides, CpG (22) in Atlantic cod SEC. Preincubation of cultured cod SECs with CpG or poly I:C selectively downregulated SR-mediated endocytosis, but only marginally affected MR-mediated endocytosis. In his tutorial presentation (A6), Clive Crossley gave an update of the invertebrate scavenger cell system, the nephrocyte, which is functionally strikingly similar to the vertebrate SEC system. He focused on insect nephrocytes that display an extensively well-developed clathrin-mediated endocytosis (23). These cells endocytose ligands that are also avidly endocytosed by the mammalian LSEC SR. At present, no information is available on the structure of these receptors. Nephrocytes produce large amounts of lactate, just as the mammalian LSEC and fish SEC do. It is assumed that this lactate is used as a high-energy fuel by neighbouring energy-demanding cells.

Molecular biology

Sergij Goerdt, in his tutorial (A3), looked for LSEC-specific features in his own work and in the literature, and found that (a) stabilin-2 is lost from non-sinusoidal hepatic endothelium late in hepatic vascular differentiation (24); (b) activation of the G-protein-coupled bile acid receptor (Gpbar1/TGR5) by bile salts leads to overexpression/activation of eNOS and enhanced NO production mediating sinusoidal relaxation and hepatic stellate cell (HSC) quiescence. In contrast, endothelin (ET)-1 induces LSEC constriction and defenestration (25–28); (c) insulin is an important LSEC growth factor cross-activating the VEGF pathway (29). Moreover, endocytosis/intracellular trafficking was recently shown to be distinct in LSECs compared with other cells (30). The LSEC-specific features are as follows: (a) a remarkable net-like distribution of clathrin heavy chain, fully associated with microtubules, but not with actin; (b) clathrin-coated vesicles only partially colocalized with early endosome antigen 1 and adaptor protein 2; (c) Wnt2, an autocrine growth and differentiation factor specific for LSECs that synergizes with the VEGF signalling pathway to exert its effects (31). As a strategy to study the specialized differentiation parameters of LSECs, highly purified LSECs and lung microvascular endothelial cells (LMECs) were compared with respect to gene expression. It was found that 319 genes are overexpressed (> 4-fold) in LSECs. Interestingly, the expression of stabilin-1 and -2 were about 25 and 1000 times higher in LSECs, whereas the von Willebrand factor was 100 times higher in LMECs.

Ageing

Old age is associated with substantial thickening and defenestration of the LSEC, sporadic deposition of collagen and basal lamina in the extracellular space of Disse and increased numbers of fat-engorged, non-activated HSCs (32, 33) (A10–13). Defenestration is also apparent in isolated LSECs (A10). There is perisinusoidal upregulation of the von Willebrand factor, VEGFR-2, collagen I and IV and intercellular adhesion molecule (ICAM)-1, and reduced expression of caveolin-1 and F-actin (32). There is a 35% reduction in sinusoidal perfusion and five-fold increase in leucocyte adhesion (33) (A12). Unlike most liver diseases, there is no change in the expression of α-smooth muscle actin (α-SMA), desmin or VEGF, reduced expression of caveolin-1 and HSCs are not activated (32) (A11). These age-related changes have been termed pseudocapillarization. Pseudocapillarization is reversed by caloric restriction and resveratrol (A48). Defenestration leads to impaired transfer of lipoproteins and provides a novel mechanism and therapeutic

target for age-related dyslipidaemia (8) (A11, 13). Old age is associated with impaired endocytic capacity by the LSEC (33) (A10, 12).

Microcirculation

LSECs originate between the 4th and the 6th gestational week from the vitelline veins and/or the septum transversum. Initially, LSECs are non-fenestrated and continuous with a basal lamina; they then differentiate into fenestrated LSECs between 10 and 17 gestational weeks (34). Transgenic mice with selective hepatic impairment of VEGF transduction have severely disrupted sinusoidal endothelium, indicating that VEGF is a pivotal cytokine in sinusoidal development (6). Cultures of fetal rat LSECs confirmed the role of VEGF and also of TGF-β1 in fetal LSEC development (A16). After development, the liver architecture is best described by hepatic microvascular subunits, the group of sinusoids supplied by a single inlet venule (35).

The responses of the microcirculation to many toxicants are similar. Initially, LSECs become swollen, develop large gaps that can lead to extravasation of erythrocytes into the space of Disse, and in severe toxicity, LSECs disintegrate and become detached debris (35–37). NO donors or metalloproteinase inhibitors ameliorate damage (36). Changes in the microcirculation occur in many chronic liver diseases. In non-alcoholic fatty liver disease, there is disruption of sinusoidal blood flow (38). Initially, this is generated by hepatocytes swollen by lipid droplets (LDs) narrowing the sinusoidal lumen. Microvascular impairment and trapping of leucocytes might contribute to HSC activation. Steatohepatitis leads to defenestration and capillarization of the LSEC with further impairment of blood flow (38). In primary biliary cirrhosis, there is aberrant expression of aquaporin-1 on the LSEC membrane, suggesting that this water channel may have a role in the development of capillarization (A14).

Role of oxygen tension

Tissue hypoxaemia is common under several pathological conditions, and LSECs are the primary targets of ischaemia-reperfusion injury following liver preservation. Hypoxia induces profound changes in the cellular gene expression profile. A major transcription factor family activated by hypoxia, hypoxia-inducible factor (HIF), contributes to the molecular regulation of the hypoxic response. High blood alcohol levels are accompanied by hypoxia and activation of HIF-1α in the liver. Ethanol increases the mRNA expression of chemokine genes (MCP-1, RANTES and MIP-2), vasoconstrictor molecules (ET-1) and HIF-1α, and activates ET-1 via HIF-1α, independent of hypoxia. The ethanol-mediated release of ET-1 may activate HSCs and exaggerate vasoconstriction and hepatic blood flow, and inflammation in the liver (A8).

The normal oxygen tension in the hepatic sinusoids is considerably lower than the atmospheric oxygen tension. Cultivation of LSECs under 5% (normoxic) oxygen tension, as opposed to hyperoxia (20%), which is used in most incubators, improved the survival of LSECs and SR-mediated endocytosis, reduced the production of interleukin (IL)-6 and increased the production of IL-10. Under normoxia, generation of H_2O_2 was reduced drastically. Thus, the viability, structure and many of the essential functional characteristics of isolated LSECs are clearly better preserved when the cultures are maintained under more physiological oxygen levels (1) (A9).

Development

Embryonic development of the liver is closely associated with vascular organization. Co-expression of SE-1 (24, 39, 40) and stabilin-2 is an adequate marker for differentiated LSECs, and both molecules are co-expressed in LSECs at the late stage of liver development (E15.5–17.5). After culturing E13.5 fetal liver cells for 7 days in the presence of VEGF, the proliferated endothelial sheets expressed neither SE-1 nor stabilin-2. In the presence of both VEGF and SB-431542 (an inhibitor of TGF-β1 receptor kinase; ALK-5), the endothelial sheets started to express stabilin-2 and contained some SE-1 co-expressing cells. These findings suggest that VEGF plays a role in the endothelial sheet formation, and blocking of TGF-β1 signalling may be involved in the differentiation of LSECs (24) (A16).

Kupffer cells

Role of Kupffer cells in alcoholic and non-alcoholic liver disease

Alcoholic liver disease (ALD) and non-alcoholic steatohepatitis (NASH) are common forms of liver disease that are histologically indistinguishable (41). Approximately 20% of alcoholics will develop ALD, while the prevalence of NASH in obese adults has been estimated at 40–100% (41). The progression of ALD and NASH is a complex process involving both parenchymal and non-parenchymal cells in the liver. There is growing appreciation for the role of the KC in both ALD and NASH.

Activation of Kupffer cells in alcoholic liver disease and non-alcoholic steatohepatitis

Chronic ethanol consumption, in both animal models and humans, increases circulating endotoxins (41, 42). Endotoxin also increases in both high-fat diet and methylcholine-deficient diet (MCD) models of NASH (1). Activation of Toll-like receptor (TLR)-4 signalling by endotoxin increases the production of inflammatory cytokines and reactive oxygen species (ROS). Mice lacking TLR-4 or CD14 are protected from both ethanol-induced and high-fat-diet-induced liver injury (41, 43).

Toll-like receptor-4 signalling is mediated by MyD88-dependent and -independent pathways. Interestingly, while TLR-4$^{-/-}$ mice are protected from ethanol-induced liver injury, MyD88$^{-/-}$ mice develop hepatic steatosis and increased alanine aminotransferase (44). In contrast, TIR-domain-containing adapter-inducing interferon (TRIF)$^{-/-}$ mice are protected from ethanol-induced liver injury (45). No studies have yet tested the differential roles of MyD88 and TRIF in models of NASH, but such studies would probably provide insights into the comparative pathophysiology of ALD and NASH.

Pro- and anti-inflammatory mediators regulating Kupffer cell activity: NADPH oxidase

Chronic ethanol feeding also sensitizes KCs to activation by lipopolysaccharides (LPS) (43). Increased production of ROS via NADPH oxidase contributes to increased LPS-stimulated ERK1/2 and p38 activation, as well as tumour necrosis factor (TNF)-α expression, in KCs from ethanol-fed rats (46) (A18). These data are consistent with the protection of p47$^{phox-/-}$ mice from ethanol-induced liver injury (43). In contrast, NADPH oxidase may not be as important in NASH as it is in ALD.